J. Basic. Appl. Sci. Res., 2(9)9594-9602, 2012

ISSN 2090-4304
Journal of Basic and Applied Scientific Research
www.textroad.com

A Coupled Computational Fluid Dynamics and Population Balance Model for Two-Phase Flow in Pipes

Mahmood Reza Rahimi, Soleiman Mosleh

Chemical engineering department, Yasouj University, Yasouj, 75918-74831, Iran

ABSTRACT

A coupled CFD-PBM model is presented for modeling turbulent two-phase bubbly flows in circular pipes. The Hydrodynamics and turbulent characteristics of air-water flow in vertical pipe is investigated. Voidage, liquid velocity and the turbulent anisotropy profiles are calculated and compared against experimental data from literature. The main aim of this work is to examine the ability of proposed coupled CFD-PBM model, especially to study packing and coring phenomena and the influence of the isotropic turbulence models on performance of CFD-PBM models. Void fraction profile gives a distinct peak near the wall and this means bubbles tended to migrate toward the wall. The weakness of isotropic turbulence models in the near wall region for two-phase flows is mentioned.
KEY WORDS: CFD, Bubbly flow, Vertical pipe, Population balance modeling.

1. INTRODUCTION

Vertical oriented two-phase flows in pipes are usually classified into basic flow regimes consisting bubbly flow, slug flow, churn turbulent flow and annular flow. In the bubbly flow, liquid is continuous phase, small dispersed bubbles flow within the liquid. The uncertainty in bubbly flow arise from a lack of deep understanding of the local hydrodynamics and rate processes, which govern bubble size and thus the interfacial area between phases.

The bubble size distribution plays an important role in the phase structure and interphase forces, which affect the multiphase hydrodynamic behaviors, including the spatial profiles of the gas fraction, gas and liquid velocities, and mixing and mass-transfer between phases. These influences must be taken into account for obtaining good predictions in wide operating conditions when using computational fluid dynamics (CFD) simulation. The population balance model (PBM) is an effective technique to simulate the bubble size distribution. An additional set of transport equations were solved to follow the prescribed discrete bubble sizes, coupling of these equations with the flow equations was performed during the simulations. Few attempts have been reported on the modeling of turbulent two-phase bubbly flows [1-9]; most of these efforts were focused on the evaluation of different models for interphase forces, especially lift and wall lubrication forces. The isotropic k-ε model has been used in many of the published works, but the influences of the isotropic models on performance of CFD models were not investigated. The main aim of this work is to examine the ability of proposed coupled CFD-PBM model, especially to show packing and coring phenomena. In this study turbulent bubbly air/water two-phase flows in a circular pipe were investigated. The internal phase distribution of air-water bubbly flow in a 57.15 mm diameter 3.06 m length vertical pipe has been modeled using the 3-D Eulerian-Eulerian multiphase flow approach coupled with Population Balance Modeling (PBM). Important flow quantities such as local void fraction, liquid velocity and the turbulent anisotropy were calculated and compared against experimental data of Wang et al. [10].

2. MODELING

The dispersed gas and the continuous liquid phases are modeled in the Eulerian-Eulerian frame work as two interpenetrating phases having separate transport equations. The governing equations without interface heat and mass transfer can be written as follows.

2.1. Continuity equations

Continuity equation of the liquid phase and gas phase with a source term that takes into account the death and birth of bubbles due to coalescence and break-up processes.

***Corresponding Author:** Soleiman Mosleh, Chemical engineering department, Yasouj University, Yasouj, 75918-74831, Iran, E-mail address: mosleh_pa@yahoo.com, Telefax: +98-7412221711

Gas phase:

$$\frac{\partial}{\partial t}(\rho_g \alpha_g f_i) + \nabla.(\rho_g \alpha_g \mathbf{u}_g f_i) = S_i \quad (1a)$$

Liquid phase:

$$\frac{\partial}{\partial t}(\rho_l \alpha_l) + \nabla.(\rho_l \alpha_l \mathbf{u}_l) = 0 \quad (1b)$$

In these equations f_i is the void fraction of bubbles of group i and Si is a source term that including the death and birth of bubbles caused by coalescence and break-up processes. $S_i = 0$ under the assumption of constant and uniform bubble size and zero interphase mass transfer. Here the term S_i is calculated as

$$S_i = P_i^B + P_i^C - D_i^B - D_i^C \quad (3)$$

and i varies from 1 to N (i =1,2,...,N) and P^B,P^C,D^B and D^C are respectively, the 'birth' and 'death' due to break-up and coalescence of bubbles. The production rates due to coalescence and break-up and the death rate due to coalescence and break-up of bubbles formulated as

$$P_i^C = \frac{1}{2}\sum_{k=1}^{N}\sum_{l=1}^{n} \chi_{i,kl} n_i n_j \quad (4a)$$

$$D_i^C = \sum_{j=1}^{n} \chi_{ij} n_i n_j \quad (4b)$$

$$P_i^C = \sum_{j=1}^{n} \Omega(V_j : V_i) n_j \quad (4c)$$

$$D_i^B = \Omega_i n_i \quad (4d)$$

n_i is the bubble number density related to the gas void fraction αg by $\alpha_g f_i = n_i V_i$ where V_i is the corresponding volume of a bubble of group i. The break-up of bubbles in turbulent dispersions employs the model developed by Luo and sevendsen [11] and the coalescence rate considering turbulent collision by Prince and Blanch [12].

2.2. Momentum conservation equations

The momentum conservation for multiphase flows is described by the volume averaged momentum equation as follows, where in which the total interfacial force acting between two phases is the sum of several independent physical effects

Gas phase:

$$\frac{\partial}{\partial t}(\rho_g \alpha_g u_g) + \nabla.(\rho_g \alpha_g u_g u_g) = -\alpha_g \nabla p + \rho_g \alpha_g g - \nabla(\tau_g \alpha_g) + F_{gl} \quad (5a)$$

Liquid phase:

$$\frac{\partial}{\partial t}(\rho_l \alpha_l u_l) + \nabla.(\rho_l \alpha_l u_l u_l) = -\alpha_l \nabla p + \rho_l \alpha_l g - \nabla(\tau_l \alpha_l) - F_{gl} \quad (5b)$$

Where $\mathbf{u}$ is the volume averaged velocity vector, p is the pressure, g is the gravity, τ is the phase shear stress tensor and F_{gl} is the interphase force term. The terms on the right-hand side describes the following forces acting on the phase k: the pressure gradient, gravity, and the viscous stress term and interphase momentum forces combined in F_{gl}. The pressure is defined to be equal in both phases. The effective viscosity μ_k of the viscous stress term consists of the laminar viscosity and an additional turbulent part in case of turbulence. The total interfacial force acting between two phases is the sum of several independent physical effects:

$$F_{gl} = F_D + F_L + F_{VM} + F_{WL} + F_{TD} \quad (6)$$

Where **u** is the volume averaged velocity vector, p is the pressure, g is the gravity, τ is the phase shear stress tensor and F_{gl} is the interphase force term. The terms on the right-hand side describes the following forces acting on the phase k: the pressure gradient, gravity, and the viscous stress term and interphase momentum forces combined in F_{gl}. The pressure is defined to be equal in both phases. The effective viscosity μ_k of the viscous stress term consists of the laminar viscosity and an additional turbulent part in case of turbulence. The total interfacial force acting between two phases is the sum of several independent physical effects:

$$F_{gl} = F_D + F_L + F_{VM} + F_{WL} + F_{TD} \quad (7)$$

The forces indicated above respectively represent the interphase drag force F_D, lift force F_L, virtual mass force F_{VM}, wall lubrication force F_{WL}, and turbulence dispersion force F_{TD}. In this model the drag force, lift force, wall lubrication force and turbulence dispersion forces are considered into account.

2.2.1. Drag force

The drag force density is written in the following form:

$$F_D = \frac{3}{4} C_D \alpha_d \rho_l \frac{1}{d_b} |u_l - u_g| (u_l - u_g) \quad (8)$$

Where C_D is the drag coefficient taking into account the character of the flow around the bubble and db is the bubble diameter. The drag coefficient C_D in Eq. (8) has been modeled using drag model of Grace [13].

2.2.2. Lift force

The lift force considers the interaction of the bubble with the shear field of the liquid. It acts perpendicular to the main flow direction and is proportional to the gradient of the liquid velocity field. The lift force in terms of the slip velocity and the curl of the liquid phase velocity can be modeled as [14-17]:

$$\mathbf{F}_L^l = -\mathbf{F}_L^g = C_L \alpha_g \rho_l (\mathbf{u}_l - \mathbf{u}_g) \times \nabla \times \mathbf{u}_g \quad (9)$$

Where C_L is the lift coefficient determined using Tomiyama model [18], which is Eötvos number dependent:

$$C_L = \begin{cases} \min[0.2888 \tanh(0.121 \mathrm{Re}), f(Eo_g)] & EO_g < 4 \\ f(Eo_g) & 4 \le EO_g \le 10 \\ -0.27 & EO_g > 10 \end{cases} \quad (10)$$

Where the Eötvos number function is defined as:

$$f(Eo_g) = 0.00105 Eo_g^3 - 0.0159 Eo_g^2 - 0.0204 Eo_g + 0.474 \quad (11)$$

Here Re is the local Reynolds number of the gas phase (bubbles) and Eo_g is the modified Eötvos number of the gas phase:

$$d_H = d_b (1 + 0.163 Eo^{0.757})^{1/3} \quad (12)$$

And db is Sauter mean diameter of bubbles, and Eötvos number is:

$$Eo = \frac{g(\rho_l - \rho_g) d_b^2}{\sigma} \quad (13)$$

2.2.3. Turbulent dispersion force

The turbulent assisted bubble dispersion, the turbulent dispersion force expression in terms of Favre-averaged variables proposed by Burns et al. [20] is used as

$$\mathbf{F}_{TD}^l = -\mathbf{F}_{TD}^g = -C_{TD} C_D \frac{\upsilon_{t,g}}{\sigma_{t,g}} \left(\frac{\nabla \alpha_l}{\alpha_l} - \frac{\nabla \alpha_g}{\alpha_g} \right) \quad (14)$$

Where C_{TD}, C_D, $\upsilon_{t,g}$, $\sigma_{t,g}$ are respectively, turbulent dispersion coefficient, drag force coefficient, turbulent kinematic viscosity of gas and turbulent Schmidt number of gas phase. The default values of C_{TD}=1 and $\sigma_{t,g}$=0.9 where used.

2.2.4. Wall lubrication force

Due to surface tension, the lateral force is formed to prevent bubbles from attaching on the solid wall resulting in a low gas void fraction nearby the solid wall and so liquid flow rate between bubble and the wall is lower than between the bubble and the outer flow. This force is known as wall lubrication force, which can be expressed by Antal et al. [21] model as:

$$\mathbf{F}_{WL}^{l} = -\mathbf{F}_{WL}^{g} = -\alpha_g \rho_l \frac{\mathbf{u}_r - (\mathbf{u}_r n_w) n_w)^2}{d_b} \max[C_{w1} + C_{w2} \frac{d_b}{y_W}, 0] n_W \quad (16)$$

Here y_w is the distance from the wall boundary,, d_b is the gas phase mean diameter, $\mathbf{u}_r=\mathbf{u}_l-\mathbf{u}_g$ is the relative velocity between phases,and nw is the unit outward normal to the wall. The model constants Cw1=-0.0064 and Cw2=0.016 where proposed by Krepper et al. [22]. The force is set to zero if the wall distance satisfies the following condition: $yw>(C_{w2}/C_{w1})d_b$ .The local Sauter mean diameter of bubbles based on the calculated values of the scalar fraction fi and discrete bubble sizes di can be deduced from:

$$d_b = \frac{1}{\sum f_i / d_i} \quad (17)$$

2.3. Turbulence modeling

Turbulence is taken into consideration for the liquid (continuous) phase using k- ε model. The principal equations for the turbulent kinetic energy k and turbulent dissipation ε are:

$$\frac{\partial}{\partial t}(\rho_l \alpha_l k) + \frac{\partial}{\partial x_i}.(\rho_l \alpha_l u_l k) = \frac{\partial}{\partial x_i}(\alpha_l (\mu_l + \frac{\mu_{l,tur}}{\sigma_k}) \frac{\partial k}{\partial x_i} + \alpha_l (G - \alpha_l \rho_l \varepsilon_l) \quad (18a)$$

$$\frac{\partial}{\partial t}(\rho_l \alpha_l \varepsilon_l) + \frac{\partial}{\partial x_i}.(\rho_l \alpha_l u_l \varepsilon_l) = \frac{\partial}{\partial x_i}(\alpha_l (\mu_l + \frac{\mu_{l,tur}}{\sigma_\varepsilon}) \frac{\partial \varepsilon_l}{\partial x_i}) + \alpha_l \frac{\varepsilon_l}{k}(C_{\varepsilon 1} G - C_{\varepsilon 2} \alpha_l \rho_l \varepsilon_l) \quad (18b)$$

$$\mu_{l,tur} = C_\mu \rho_c \frac{k_c^2}{\varepsilon_c} \quad (18c)$$

G is the turbulence production term. The values of standard $k-\varepsilon$ model constant $C_{\varepsilon 1}$, $C_{\varepsilon 2}$, C_μ, σ_k, σ_ε are: $C_{\varepsilon 1}=1.44$, $C_{\varepsilon 2}=1.92$, $C_\mu=0.09$, $\sigma_k=1$, $\sigma_\varepsilon=1.3$.

For the gas phase no turbulence model was used. The influence of the gas (dispersed) phase on the turbulence of the liquid (continuous) phase is taken into account with the Sato's bubble-induced turbulent viscosity model [23], therefore

$$\mu_{\alpha,eff} = \mu_{\alpha,lam} + \frac{\mu_{\alpha,tur}}{\sigma_k} + \mu_s \quad (19)$$

2.4. Coupling CFD and PBM

The two-way coupling between computational fluid dynamics (CFD) and population balance model (PBM) was implemented in the model. The bubble size distribution is divided into a number N of discrete size classes, while it is assumed that bubbles of all sizes have a common velocity field, where the Sauter mean diameter influences the drag term. The Sauter mean diameter of the bubbles is calculated in each time step and returned to the drag force in Eq. (7). All bubble diameter classes have the same velocity in this homogeneous population balance model evaluated at the Sauter mean diameter, therefore Navier–Stokes equations is solved for all bubble classes.

The turbulent energy dissipation and the void fraction required in the source terms for coalescence and breakage is returned for each cell from the solver. The dispersed phase velocity is derived from the Navier–Stokes equations.

3. SOLUTION METHOD AND VALIDATION OF MODEL

The work performed by Wang et al. [10] was used to check the capabilities of the model proposed for isothermal vertical bubbly flow in pipes. An air-water loop was used by Wang et al. [10] had a 57.15 mm

internal diameter and 3.06 m length test section for measurements of both up- and down-flows. A single sensor cylindrical hot-film probe was used to measure the mean and fluctuations in the axial liquid velocity and the local void fraction. Reynolds stress components in the liquid phase, measured using a special 3-D conical probe.

One eighth of a vertical pipe using symmetry boundary conditions for both axial cut planes was used in order to reduce the computational costs. The first layer in inflated layer near the wall was set at a distance from the wall to take a value of the y+ in the range from 30 to 40, in order to achieve stable solutions avoiding numerical oscillations and also to have an accurate wall lubrication force modeling.

The simulations were carried out as 3-D up-flow in a vertical pipe based on the two-fluid Eulerian–Eulerian approach combined with Population Balance Modeling (PBM). Conservation equations are discretised using finite volume method, high resolution scheme was used for all equations, SIMPLEC algorithm was used for pressure-velocity coupling. Water was considered as the continuous phase, and air as the dispersed phase. In this study, bubbles are equally divided into 5 classes. The PBM model has been used to account for the non-uniform bubble size distribution in a gas–liquid mixture.

The following boundary conditions were used in this study. For the pipe inlet boundary condition, uniform gas and liquid velocities and average volume fractions have been specified; a relative average static pressure of zero was specified at the pipe outlet boundary condition. Symmetry boundary conditions were used for both axial cut planes. No slip boundary conditions were used at wall. Average void fraction and uniform liquid velocity profile are specified for initiating the numerical solution. Several grids were used in order to set up the computational domain. The best computational time and also independency of the results from the calculation grid was examined for different grids. Several simulations were done using gradually larger number of grid points starting from about 30000, there was seen practically no change in the gas void fraction and liquid velocity profiles when the number of grid numbers increased beyond 120000. The mathematical model was applied in the CFD commercial code for numerical studies, with the construction of a particular numerical grid and with its own subroutine in Fortran language for the closure equations of model.

3. RESULTS AND DISCUSSION

The proposed model was tested by using the model for an air/water flow system used by Wang et al. [10]. The predicted values of gas void fraction were presented in Fig. 1 for different values of superficial gas and liquid velocities. This figure shows the void fraction distributions obtained from the model comparing against experimental data at the dimensionless axial position z/D = 35, the results are follows the correct trend, as can be seen in this figure. It was found that the void fraction profile showed a distinct peak near the wall that means bubbles tended to migrate toward the wall. From the phenomenological view point, the phase distribution patterns along the radial direction exhibits four basic types of distributions: “wall peak”, “intermediate peak”, “core peak” and “transition”, as categorized by Serizawa and Kataoka [12]. In the bubbly flow regime, maximum void fraction located close to the wall demonstrated the flow phase distributions typically known as the “wall peak” behavior, this phenomenon was discussed by wang et al. [10], they stated that positive lift force pushing the small bubbles toward the pipe wall. As depicted in Fig. 1, a well-developed wall peaking behavior was recorded in the experiment and had been successfully captured by the model. For higher liquid flows it was found that "wall-peaking" became more pronounced. The results are shown that peaking and coring of gas void fraction is well-predicted using this combined CFD- PBM model of this study. The predictions are in good agreement with experimental data, but the discrepancy occurred close to the wall.

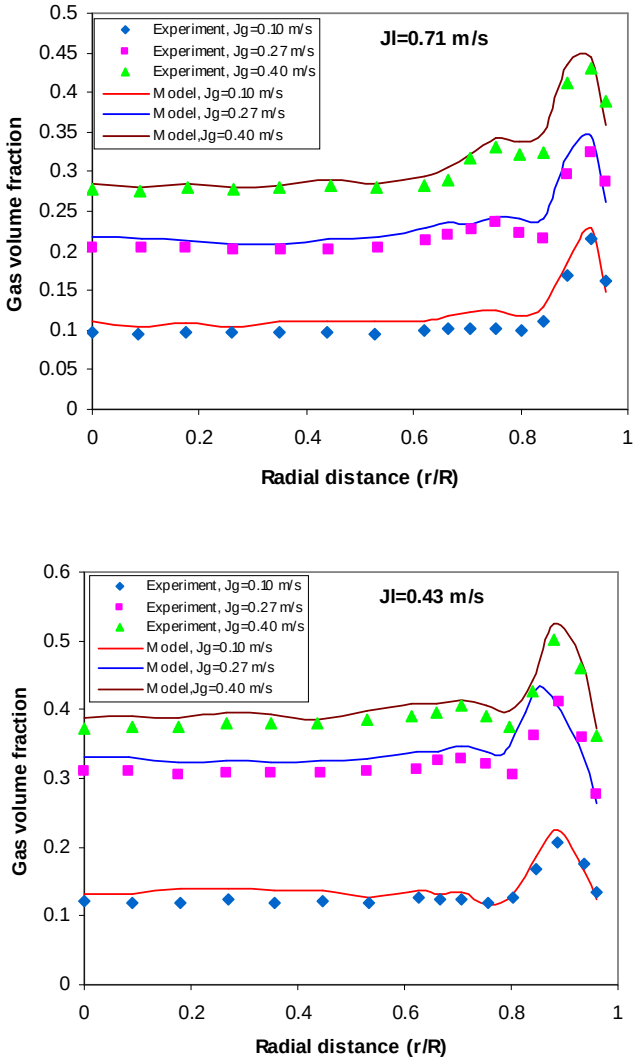

Figure 1. Gas void fraction in comparison with experimental data of Wang et.al.[10].

Fig. 2 shows the local radial liquid velocity distributions at z/D = 35 for two superficial liquid velocities and three gas superficial velocities. As depicted in Fig. 3 the simulation results of liquid velocity profiles are compared with experimental data and good agreement with the experimental data was found, although the liquid velocities at the core were over-predicted.

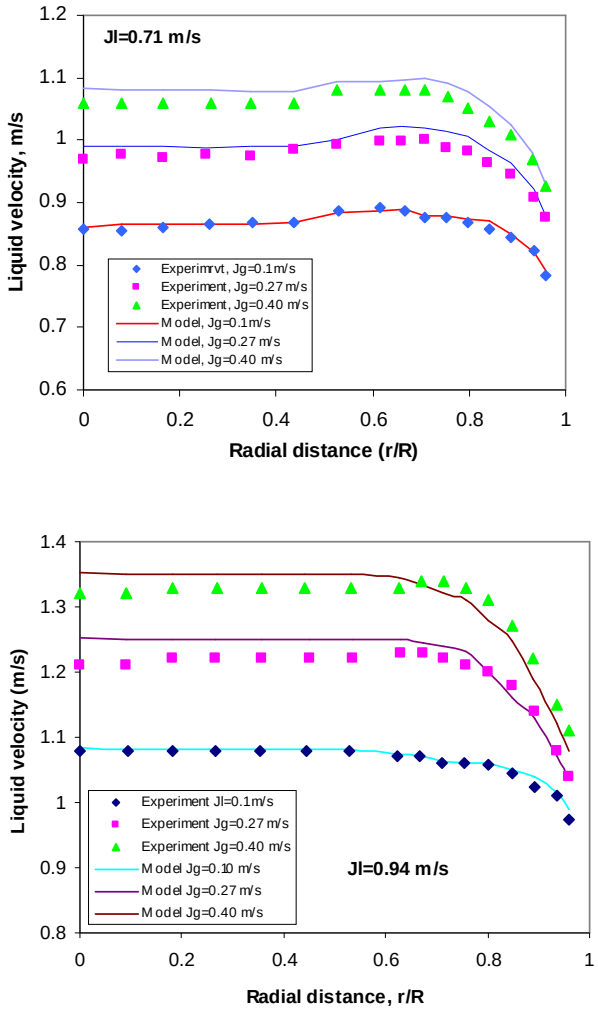

Fiqure 2. Local radial liquid velocity distributions at z/D = 35.

A primary objective of this study is to investigate the influence of turbulence model in predicting two-phase flows. The experimental RMS values of turbulent velocity were compared against the predicted values. Also, all two-equation models assume isotropy of turbulence, i.e. the velocity fluctuations are supposed to be equal in magnitude. Despite these uncertainties certain useful results can be obtained from the results, a sample of which is included here. Fig. 3 shows turbulence anisotropy data of Wang et al. [10] compared with isotropic turbulence value. This figure is shown carefully that isotropic assumption and therefore use of isotropic turbulence models is under question for near wall regions, although the overall results are acceptable in engineering (overall) point of view. The experimental observations were shown that turbulent fluctuation in axial direction is at least one order of magnitude greater than other directions [10]. It is evident that using isotropic turbulence models introduced some errors in prediction of near wall effects, whereas high shear flows exist in those regions. In coupling of CFD and PBM as aforementioned above the turbulent energy dissipation and the void fraction required in the source terms for coalescence and breakage is returned for each cell from the solver. Therefore the weakness of isotropic turbulence model in the near wall regions can be the main source of error in near wall prediction.

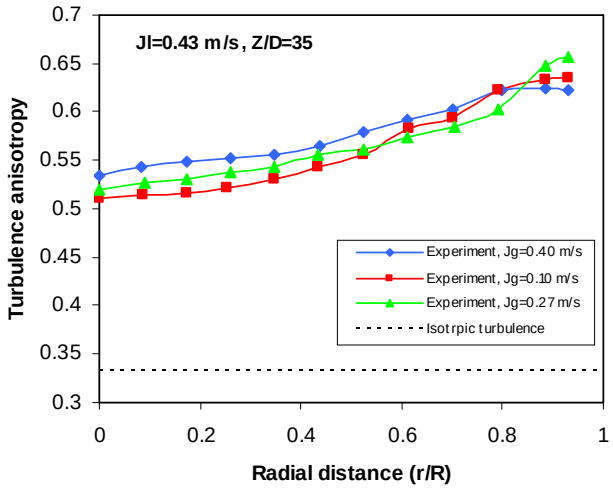

Figure 3. Turbulence anisotropy in comparison with measured data of Wang et al.[10], z/d=35.

Moreover, for high flows in the upward direction the location of the maximum liquid velocity occurred off the pipe's centerline. But the maximum liquid velocity and the gas void fraction peak did not occur at the same location, Wang et al.[10] believed that this phenomenon is probably because of the counteracting effect of high shear stress near the wall as shown by. However the maximum liquid velocity occurs away from the pipe's centre, which observed experimentally [10] and named "chimney effect".

5. Conclusion

The ability of coupled CFD-PBM model, especially for showing packing and coring phenomena and the influence of the isotropic turbulence models on performance of CFD-PBM model - for turbulent bubbly air-water two-phase flows in a circular pipe - were investigated. Significant flow quantities such as local void fraction, liquid velocity and the turbulent anisotropy were calculated and compared against experimental data of Wang et al. [10]. The void fraction profile is shown a sharp peak near the wall. The maximum liquid velocity occurs away from the pipe's center, which is a "chimney effect". In the core region the void fraction commonly showed flat profiles.

The results was shown carefully that isotropic turbulence assumption and therefore using isotropic turbulence models is under question for near wall regions, although the overall results are acceptable in engineering (overall) point of view. Therefore the weakness of isotropic turbulence model in the near wall regions can be the main source of error in near wall prediction of this model.

REFRENCES

(1) Kocamustafaogullari G, Ishii M (1995). Foundation of the interfacial area transport equation and its closure relations. Int. J. Heat Mass Trans. 38 (3), 481–493.

(2) Hibiki T, Ishii M (2002). Development of one-group interfacial area transport equation in bubbly flow systems. Int. J. Heat Mass Trans. 45, 2351–2372.

(3) Hibiki T, Ishii M, Xiao Z (2001). Axial interfacial area transport of vertical bubble flows. Int. J. Heat Mass Trans. 44, 1869–1888.

(4) Ekambara K, Sanders RS, Nandakumar K, Masliyah JH (2008). CFD simulation of bubbly two-phase flow in horizontal pipes, Chem. Eng. J. 144, 277–288.

(5) Wang T, Wang J, Jin Y (2005). Population Balance Model for Gas−Liquid Flows: Influence of Bubble Coalescence and Breakup Models, Ind. Eng. Chem. Res., 44, 19.

(6) Cheung CP, Yeoh GH, Tu JY (2007) On the modeling of population balance in isothermal vertical bubbly flows – Average bubble number density approach. Chem. Eng. Process. 46 (8), 742–756.

(7) Sarı S, Ergün S, Barık M, Kocar C, Sökmen CN (2009). Modeling of isothermal bubbly flow with ınterfacial area transport equation and bubble number density approach, Annals of Nuclear Energy, 36, 222-232.

(8) Ghorai S, Nigam KDP (2006) CFD modeling of flow profiles and interfacial phenomena in two-phase flow in pipes, Chemical Engineering and Processing: Process Intensification, 45, 1, 55-65.

(9) Dhotre MT, Smith BL, Niceno B (2007) CFD simulation of bubbly flows: Random dispersion model, Chemical Engineering Science, 62, 24,7140-7150.

(10) Wang SK, Lee SJ, Jones OC, Lahey RT (1987). 3-D turbulece structure and phase distribution measurements in bubbly two-phase flows, Int. J. Multiphase flow, 3, 327-343.

(11) Luo H, Svendsen H (1996). Theoretical model for drop and bubble break-up in turbulent dispersions, AIChE J. 42, 1225–1233.

(12) Prince MJ, Blanch HW (1990). Bubble coalescence and break-up in air sparged bubble columns, AIChE J. 36 1485–1499.

(13) Grace JR, Clift R, Weber ME (1978) Bubbles, Drops and Particles, Academic Press.

(14) Zun I (1980). The transverse migration of bubbles influenced by walls in vertical bubbly flow, Int. J. Multiphase Flow 6, 583–588.

(15) Thomas NH, Auton TR, Sene K, Hunt JCR (1983). Entrapment and transport of bubbles by transient large eddies in turbulent shear flow, in: BHRA International Conference on the Physical Modeling of Multiphase Flo.

(16) Drew DA, Passman SL (1999). Theory of Multicomponent Fluids, Springer-Verlag, New York, NY.

(17) Tomiyama A, Tamai H, Zun I, Hosokawa S (2002). Transverse migration of single bubbles in simple shear flows, Chem. Eng. Sci. 57, 1849–1858.

(18) Tomiyama, A (1998). Struggle with computational bubble dynamics, 3rd International Conference on Multiphase Flow, ICMF-2004, Lyon, France, June 8–12, 1998, 1–18.

(19) Wellek RM, Agrawal AK, Skelland AHP (1966). Shapes of liquid drops moving in liquid media. AIChE J. 12, 854.

(20) Burns AD, Frank T, Hamill I, Shi J (2004). The Farve averaged drag model for turbulent dispersion in Eulerian multi-phase flows. In: Proceeding of the Fifth International Conference on Multiphase flow, Yokohama, Japan.

(21) Antal SP, Lahey RT, Flaherty JE (1991). Analysis of phase distribution in fullydeveloped laminar bubbly two phase flow, Int. J. Multiphase Flow, 7, 635.

(22) Krepper E, Lucas D, Prasser HM (2005). On the modelling of bubbly flow in vertical pipes, Nuclear Engineering and Design 235, 597–611.

(23) Sato Y, Sadatomi M, Sekoguchi K (1981). Momentum and heat transfer in two-phase bubbly flow—I. International Journal of Multiphase Flow, 7,167–178.